Thiol Peroxidase Deficiency Leads to Increased Mutational Load and Decreased Fitness in *Saccharomyces cerevisiae*

Alaattin Kaya,*,[1] Alexei V. Lobanov,*,[1] Maxim V. Gerashchenko,* Amnon Koren,[†] Dmitri E. Fomenko,[‡] Ahmet Koc,[§] and Vadim N. Gladyshev*,[2]

*Division of Genetics, Department of Medicine, Brigham and Women's Hospital and [†]Department of Genetics, Harvard Medical School, Boston, Massachusetts 02115, [‡]Department of Biochemistry and Redox Biology Center, University of Nebraska, Lincoln, Nebraska 68588, and [§]Department of Molecular Biology and Genetics, Izmir Institute of Technology, 35430 Urla, Izmir, Turkey

ABSTRACT Thiol peroxidases are critical enzymes in the redox control of cellular processes that function by reducing low levels of hydroperoxides and regulating redox signaling. These proteins were also shown to regulate genome stability, but how their dysfunction affects the actual mutations in the genome is not known. *Saccharomyces cerevisiae* has eight thiol peroxidases of glutathione peroxidase and peroxiredoxin families, and the mutant lacking all these genes (Δ8) is viable. In this study, we employed two independent Δ8 isolates to analyze the genome-wide mutation spectrum that results from deficiency in these enzymes. Deletion of these genes was accompanied by a dramatic increase in point mutations, many of which clustered in close proximity and scattered throughout the genome, suggesting strong mutational bias. We further subjected multiple lines of wild-type and Δ8 cells to long-term mutation accumulation, followed by genome sequencing and phenotypic characterization. Δ8 lines showed a significant increase in nonrecurrent point mutations and indels. The original Δ8 cells exhibited reduced growth rate and decreased life span, which were further reduced in all Δ8 mutation accumulation lines. Although the mutation spectrum of the two independent isolates was different, similar patterns of gene expression were observed, suggesting the direct contribution of thiol peroxidases to the observed phenotypes. Expression of a single thiol peroxidase could partially restore the growth phenotype of Δ8 cells. This study shows how deficiency in nonessential, yet critical and conserved oxidoreductase function, leads to increased mutational load and decreased fitness.

BEING hereditary material, DNA is propagated from generation to generation while maintaining genome stability in the face of random mutations. Genome instability results mainly from DNA damage and error-prone DNA synthesis, and it is crucial for any organism to properly maintain its genome and neutralize damage to it (Nishant *et al.* 2010). There are various types of agents that can cause DNA damage by modifying the structural properties of DNA, and oxidative stress is one of the best-studied factors that may affect DNA stability. Aerobic organisms inevitably produce reactive oxygen species (ROS) as a consequence of incomplete reduction of molecular oxygen during respiration, as well as by other metabolic processes. ROS may cause oxidative damage by reacting with and affecting functions of many cellular metabolites and macromolecules, including proteins, lipids, and DNA (van Loon *et al.* 2010). Continuous exposure of intracellular milieu to ROS is implicated in the etiology of various diseases, such as diabetes, neurodegeneration, and atherosclerosis. ROS are also involved in cancer development by increasing the mutation rate via oxidative DNA damage and genomic instability (Marnett 2000; Reddy *et al.* 2009). More than a hundred different types of oxidative DNA damage have been described; among them, oxidative conversion of guanine to 7,8-dihydro-8-oxoguanine (8-oxo-G) is the most prominent modification. 8-oxo-G leads to misincorporation of adenine in place of guanine, resulting in the CG→AT transversion. Spontaneous deamination of methylated cytosine is a hydrolytic modification, leading to thymine substitution, and CG→TA transitions are driven by oxidation of methylated

doi: 10.1534/genetics.114.169243
Manuscript received July 31, 2014; accepted for publication August 25, 2014; published Early Online August 29, 2014.
Supporting information is available online at http://www.genetics.org/lookup/suppl/doi:10.1534/genetics.114.169243/-/DC1.
[1]These authors contributed equally to this work.
[2]Corresponding author: Division of Genetics, Department of Medicine, Brigham and Women's Hospital and Harvard Medical School, New Research Bldg., Room 435, 77 Ave. Louis Pasteur, Boston, MA 02115. E-mail: vgladyshev@rics.bwh.harvard.edu

cytosine (van Loon *et al.* 2010). These modifications serve as markers of oxidative DNA damage and are the most common point mutations in a variety of human genetic diseases, including cancer (Cooke *et al.* 2003; van Loon *et al.* 2010).

Organisms have evolved a wide variety of defense mechanisms to prevent or limit the consequences of oxidative damage. They include two independent mechanisms of DNA repair, base excision repair and nucleotide excision repair (Degtyareva *et al.* 2008), as well as antioxidant defense systems, such as superoxide dismutase, catalase, and peroxiredoxin (Prx), which scavenge ROS (Huang *et al.* 2003). These and other systems collaborate in protecting cells from genomic instability induced by oxidative stress (Kryston *et al.* 2011). Recent studies suggest that antioxidant defense is the first line of defense against oxidative DNA damage. For example, thiol-dependent oxidoreductases prevent large-scale chromosomal rearrangements, and their deficiency leads to an increase in the mutation rate (Iraqui *et al.* 2009; Tang *et al.* 2009). These enzymes include ubiquitous thiol peroxidases containing a catalytic cysteine (Cys) residue that becomes oxidized in the process of scavenging hydrogen peroxide, alkyl hydroperoxides, and other peroxide forms (Wong *et al.* 2002). Most organisms have multiple Prxs, *e.g.*, five Prxs occur in the yeast *Saccharomyces cerevisiae*, 10 in the plant *Arabidopsis thaliana*, and six in mammals (Park *et al.* 2000; Horling *et al.* 2003; Rhee *et al.* 2005). Three glutathione peroxidases (Gpxs), members of another family of thiol peroxidases, were also identified in yeast, and eight such enzymes occur in mammals (Inoue *et al.* 1999; Brigelius-Flohe 2006). Like Prxs, Gpxs catalyze the reduction of hydrogen peroxide and other hydroperoxides, but most often use glutathione as an electron donor for these reactions (Brigelius-Flohe 2006). Both Prxs and Gpxs occur in various cellular compartments, show tissue-specific expression in mammalian cells, and differ in abundance (Brigelius-Flohe 1999; Muller *et al.* 2007; Gerashchenko *et al.* 2012).

Despite proposed roles of these antioxidant enzymes in genome stability, there is no direct information on the genome-wide mutation process and DNA stability when these functions are compromised. A recent study screened a yeast knockout library and identified individual peroxidases as mutation suppressors (Huang *et al.* 2003). Following this observation, additional studies examined mutation rates for cells lacking individual and multiple Prxs, showing that the Tsa1 null yeast cells had the strongest mutator phenotype. These studies assessed mutation rates for small marker loci such as canavanine (CAN1) and uracil (URA3), which are commonly used for fluctuation assays but have limitations for interpreting the richness, diversity, and specificity of mutation phenotypes when applied to entire genomes (Wong *et al.* 2004; Iraqui *et al.* 2009; Tang *et al.* 2009). Currently, information on the genome-wide mutational spectra of thiol peroxidase null cells is lacking.

To begin addressing the functions of thiol peroxidases in genome stability, we previously developed a model using the budding yeast *S. cerevisiae*, in which we deleted all eight thiol peroxidases (Δ8 cells) and found that deficiency in these enzymes disrupts hydrogen peroxide-dependent transcriptional regulation (Fomenko *et al.* 2011). In the present study, we developed an independent Δ8 strain and assessed how deficiency in these enzymes in two different isolates affects cellular fitness and genome stability. We also subjected Δ8 and wild-type (WT) cells to a long-term mutation accumulation (MA) experiment. Genome sequencing of Δ8 isolates as well as various MA lines revealed that thiol peroxidases are important factors for genome maintenance. We describe several hypermutability regions in a pattern of clustered mutations in Δ8 cells, which are extended up to 150 kb. These data suggest that the lack of thiol-based redox control leads to a distinct mutator phenotype, directly implicating thiol peroxidases in genome stability.

Materials and Methods

S. cerevisiae strains

Construction of a mutant strain lacking all eight thiol peroxidases was reported previously (Fomenko *et al.* 2011). Briefly, it was obtained by mating Prx null (Δ5Prx) (Wong *et al.* 2004) and Gpx null (Δ3Gpx) (Avery and Avery 2001) strains. The resulting diploids were analyzed by tetrad dissection; several hundred spores were checked on Yeast Nitrogen Base selection plates for histidine, leucine, uracil, and methionine auxotrophy and for G418 resistance. The growing colonies were selected, and we performed a second PCR screening for each locus with the use of *HIS3*, *URA3*, and KanMX markers. Initially, we isolated colonies lacking six or seven peroxidases, named Δ6 and Δ7, followed by deletion of the remaining one or two peroxidases to yield Δ8 cells. Details regarding the strains used can be found in Supporting Information, Table S1. Both WT cells and multiple Gpx and Prx mutants were in the BY4741 background. Yeast strains were grown on yeast extract–peptone–dextrose (YPD) medium. For respiratory growth, cells were grown on YPD containing 2% glycerol, ethanol, or lactic acid.

Phenotypic characterization of the peroxidase null strain

After growing cells for 2 days on YPD plates, individual colonies were picked for both WT and Δ8 strains, each inoculated in 10 ml of YPD liquid media and cultured overnight at 30° with moderate shaking. Overnight cultures were diluted to an OD_{600} of 0.02. Cell growth was monitored by OD_{600} measurements. YPD plates and liquid culture were supplemented with 20 μg/ml phleomycin for *TSA1*-expressed strains. Data from individual growth curves were used to calculate cell division time. For replicative aging experiments, 20 individual virgin daughter cells were collected for both WT and Δ8 cells. New buds from these original daughter cells were separated and discarded, as they were formed, using a dissecting microscope. This process continued until cells ceased dividing.

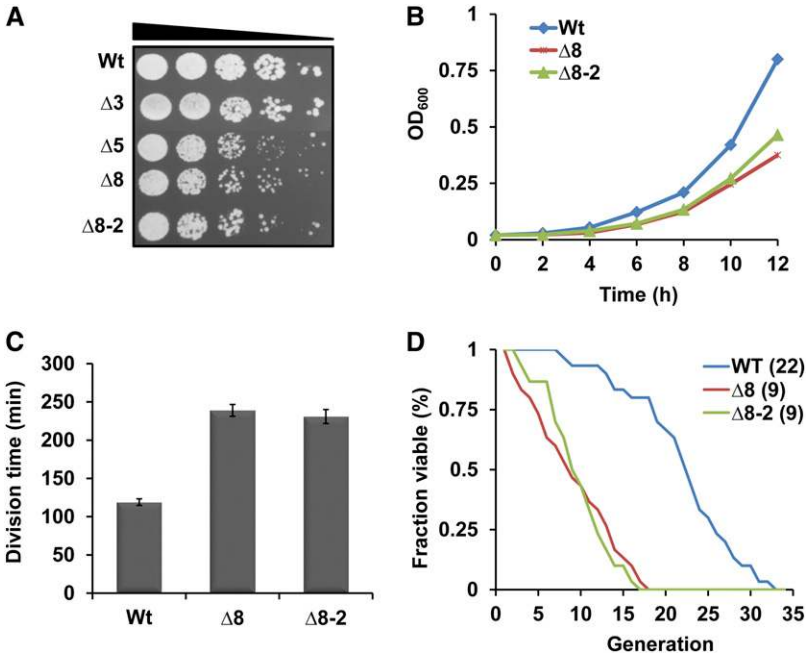

Figure 1 Deletion of eight thiol peroxidases causes growth defects and reduces life span in yeast. (A) Decreased colony growth of Δ8 cells. Overnight cultures of WT, Δ3, Δ5, and two independent Δ8 isolates were diluted to an OD_{600} of 0.3. Then, 5 μl of 10-fold dilution of each cell suspension was spotted onto YPD plates and photographed 3 days later. (B) Reduced cell growth of Δ8 cells. Growth of WT and Δ8 cells in liquid YPD medium was monitored by measuring the OD_{600}. (C) Increased division time of Δ8 cells. Division time (in minutes) was calculated for each strain and plotted. (D) Replicative life span of WT and Δ8 cells. Numbers in brackets next to each strain indicate mean life span. The *y*-axis represents the fraction of survivors (fraction of mother cells capable of budding) at each generation (*x*-axis).

Establishment of MA lines and whole-genome sequencing

MA lines were initiated from isogenic lines of WT and Δ8 strains, which were passed through 50 single-cell bottlenecks for a total of ~1500 cell divisions for WT lines and ~800 divisions for Δ8 lines over a course of 1 year. We kept the original, initial isogenic WT and Δ8 cells frozen at −80°, which were subsequently sequenced together with the MA lines. At the end of the bottleneck process, cells from the 1-year-old Δ8 and WT lines were centrifuged and kept frozen at −80°. DNA from each line was extracted using MasterPure yeast DNA purification kit (Epicenter) according to the manufacturer's protocol. For sequencing, genomic DNA samples were prepared according to the standard Illumina protocols for library preparation. Initial cells and all MA lines were paired-end sequenced with 75-bp reads on an Illumina Hi-Sequation 2000 platform.

Assembly and detection of base substitutions and small indels

Yeast reference genome was downloaded from the National Center for Biotechnology Information web site (http://ftp.ncbi.nih.gov). Sequencing reads were aligned to the reference genome using a variety of tools. The best results were obtained using Burrows–Wheeler Aligner, which utilizes a backtracking method to search for inexact matches and provides a mapping quality score for each read (Li and Durbin 2009). Further analysis was conducted using the Genome Analysis Toolkit (GATK) framework (McKenna *et al.* 2010) according to the program's manual. Comparisons with the reference genome, as well as pairwise comparisons of initial *vs.* MA lines, were performed to identify point mutation substitutions and small indels. The following additional criteria were implemented: (i) the nucleotide in question should have been covered by at least three reads and (ii) the GATK score for this position should have been >10 (which corresponds to $P = 0.001$ probability of misidentification). The data were further analyzed using a SHORE toolkit (Schneeberger *et al.* 2009), which was designed to allow a higher tolerance for diverged regions. The reported base substitutions and structural variants were then compared with the GATK output, and read alignments were manually verified with Tablet software (Milne *et al.* 2010). For each base substitution or indel candidate, location on the chromosome was analyzed. An annotation file downloaded from the *Saccharomyces* Genome Database (http://www.yeastgenome.org/) was used to determine coding and intergenic noncoding regions.

Calculation of mutation rates and analysis of mutation clusters

Mutation rate was calculated by dividing the number of detected mutations by the total number of bases in the reference genome sequence and by the number of generations that each strain was propagated. For the initial Δ8 strain, the number of generations is unknown, so we calculated the mutation frequencies only. Standard errors were calculated as the square root of mutation rate divided by the number of nucleotides in the genome and the number of generations (Denver *et al.* 2004). For MA lines 2A and 2B, mutations that were common to both lines were considered to have occurred in each of the lines. Mutation numbers for different mutation types were calculated by further normalizing mutations from AT base pairs by the AT fraction of the genome and mutations from GC base pairs by the GC fraction of the genome. Clusters were analyzed according to a previously described method (Michaelson *et al.* 2012). Details of the analysis can be found in the figure legend (Figure 3).

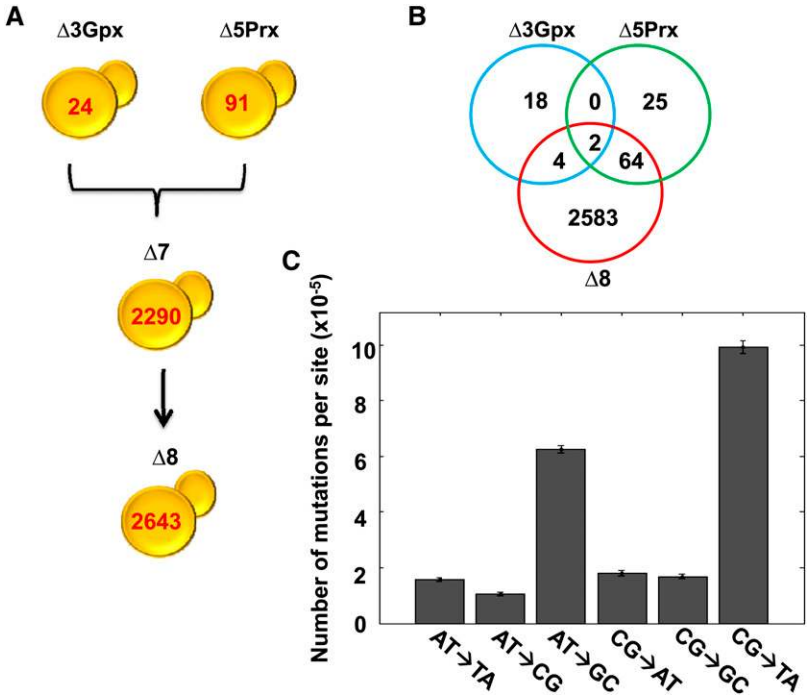

Figure 2 Quantification of mutations in multiple thiol peroxidase mutants. (A) Mutational landscape of thiol peroxidase mutants. Genome sequencing revealed 24 mutations in Δ3, 91 in Δ5, 2290 in Δ7 (all peroxidases lacking except for Gpx2), and 2643 in Δ8 cells. (B) Mutations identified in the mutant strains represented by Venn diagram. Mutation distribution is shown for three strains: Δ3 Gpx (blue), Δ5 Prx (green), and Δ8 strain (red). The number of mutations was calculated using the GATK procedure, and the common mutations were identified by comparing the sets of mutations among the strains. (C) Number of mutations of each type in the original Δ8 strain. Number of mutations was calculated by dividing the number of detected mutations by the total number of bases in the reference genome sequence.

Spot assays for genotoxin sensitivity

Resistance of WT and Δ8 strains to different genotoxic agents was assessed by spot assays. Ten microliters of WT, Δ3Gpx, and Δ5Prx cultures at the OD_{600} of 0.3 were serially diluted to fresh YPD plates containing indicated amounts of campothecin, phleomycin, benomyl, or hydroxyurea. Cells were grown for 3 days at 30°, and pictures were taken. For the Δ8 strain, the initial OD_{600} was 0.6 since the number of cells of this strain was approximately 2-fold lower in the absence of treatment.

Messenger RNA isolation and fragmentation for transcriptome analyses

Frozen yeast pellets were cryo-grinded in a BioSpec mini bead beater. Lysis was performed with solutions from a RNAqueous mini kit (LifeTech). Isolation of total RNA proceeded according to the kit manual. Messenger RNA (mRNA) was purified from total RNA using an mRNA Direct Kit (LifeTech) according to the manufacturer's guidelines. Fragmentation of mRNA was achieved by a 30-min incubation in 1 mM EDTA, 500 mM $NaHCO_3$, pH 9.2, at 95°.

Precipitation of RNA and DNA

The following components were added to the initial sample: 1/10 volume of ammonium acetate (Ambion), 5 μl of glycogen (5 mg/ml, Ambion), and 2.5 volumes of absolute ethanol. The mixture was incubated for 1 hr at −20°, and nucleic acids were precipitated by a 15-min centrifugation at 20,000 × *g*. This method was used to precipitate DNA and RNA after all enzymatic reactions.

Sequencing library preparation

mRNA fragments were treated with T4 polynucleotide kinase (Thermo Scientific) for 1 hr in 10 μl total reaction volume. RNA was loaded on a 15% TBE–urea polyacrylamide gel (Invitrogen). The band corresponding to 50–70 nt was cut out of the gel and crushed with a disposable pestle (Kimble Chase), and RNA was eluted during a 3-hr incubation at 37° in 0.3 ml of elution buffer (20 mM Tris–HCl, pH 7.0, 2 mM EDTA, 1/10 volume of 3 M ammonium acetate, 40 U/ml Superase-In). Gel particles were eliminated by a Corning Costar spin-X 0.22-μm column. RNA was precipitated. One hundred nanograms of 3′ adapter per sample were ligated by T4 RNA ligase 2 truncated KQ or K227Q (New England Biolabs). Reaction products were precipitated, and reverse transcription was set up as follows. RNA pellet was dissolved in 11.5 μl of water, and 4 pmol of reverse transcription primer was added along with 1 μl of dNTP mix (10 mM each). The mixture was incubated for 5 min at 65° and then chilled on ice. Two microliters of DTT and 4 μl of First Strand Buffer (refer to manufacturer's protocols for composition) were added along with 0.5 μl of SuperScript II and 0.5 μl Superase-In to the total volume of 20 μl. Reaction then continued for 30 min at 42°, 1 min at 65°, and 5 min at 80°. RNA was degraded in the presence of 80 mM NaOH at 95° for 30 min and then neutralized by the same amount of HCl. Reaction products were precipitated and run on 10% TBE–urea polyacrylamide gel (Invitrogen), and the band corresponding to the transcriptase extended product was cut off. DNA was eluted as described above, precipitated, and later used in a CircLigase II reaction (20 μl total volume, according to the manufacturer's instructions; Epicentre). Products of ligation were used in the final PCR without additional precipitations or purifications. PCR was set up as follows: 10 pmol reverse and forward primers (Table S3), 10 μl High Fidelity buffer, 0.5 μl Phusion polymerase (New England Biolabs), 1–4 μl of ligation product, and

water up to 50 μl. PCR mix was subjected to 6–10 cycles of amplification (94° for 15 sec, 55° for 10 sec, 65° for 10 sec). Cycling was finalized for 2 min at 65°. PCR products were precipitated and run on 8% TBE polyacrylamide gel, and the band corresponding to the amplified products was cut off. DNA was eluted as described above, precipitated, and sent for sequencing on an Illumina HiSequation 2000 platform. The data analysis was described previously (Gerashchenko *et al.* 2012).

Expression of TSA1 in WT and mutant lines

We used phleomycin (bleMX6) containing plasmid pCEV-G1-Ph (Vickers *et al.* 2013) to express the *TSA1* in WT and Δ8 strains. The entire coding sequence of *TSA1* (from start to stop codon) was amplified with specific primers containing 5′-*Not*I and 3′-*Pac*I restriction sites and cloned into a plasmid for expression under the control of yeast *TEF1* promoter. For yeast transformation, overnight cultures were diluted and grown until mid-log phase (OD_{600} = 0.6). One milliliter of each culture was used for transformation with an empty vector as control and the *TSA1*-containing construct for expression using a lithium acetate method. After transformation, cells were incubated for 3 hr at 30° and spread onto plates containing 20 μg/ml phleomycin. Colonies were chosen after 5 days and restreaked onto new plates containing either 40 μg/ml phleomycin or 100 μg/ml zeocin since the bleMX6 cassette provided resistance to both antibiotics (Vickers *et al.* 2013). Colonies, which were grown on both plates, were used for subsequent experiments.

Results

Deletion of eight thiol peroxidases leads to growth and life-span defects

Combined knockout of eight thiol peroxidases (Table S1), prepared from cells lacking three Gpxs (Δ3) and five Prxs (Δ5), was not lethal in *S. cerevisiae* cells (Fomenko *et al.* 2011), but led to several phenotypic changes (Figure 1). Thiol peroxidase deficiency yielded an approximately twofold decrease in growth rate (Figure 1C). We also measured the replicative life span of Δ8 and WT strains. The mean life span of Δ8 cells was nine divisions, approximately 2-fold lower compared to the 22 divisions observed in the WT strain (Figure 1D).

The genome of the thiol peroxidase null strain is highly unstable

To assess the role of thiol peroxidases in genome stability, we sequenced and analyzed the genomes of Δ3, Δ5, and Δ8 (Δ8 initial) strains and compared them with the genome of isogenic WT (WT initial) cells. This procedure revealed 2633 point mutations in Δ8 relative to WT cells (Figure 2A). Most of them occurred during and after construction of this strain, since only 24 mutations were observed in Δ3 cells and 91 mutations in Δ5 cells compared to the reference WT genome (Figure 2B). In the initial Δ8 cells, CG→TA and AT→GC transitions were much more common than other mutation types (Figure 2C). We examined the locations of point mutations and found that 1161 mutations were in noncoding regions. Among 1472 mutations within coding sequences, 1041 were silent (Table 1 and File S1). The initial Δ8 strain also had 11 mutations found in noncoding regions (9 base substitutions and 2 insertions) of the mitochondrial genome. To test for a possible change in mitochondrial function, we analyzed the respiratory function by growing cells on ethanol, glycerol, and lactic acid and found that the Δ8 strain can utilize these substrates (Figure S1). Mutations found in the coding region of the genome were distributed among 261 genes, with 149 genes having more than one mutation. Most genes with multiple mutations coded for cell-wall proteins rich in multiple tandem repeats. A putative chloride transporter (YHL008C) had the highest number of mutations (196 mutations), followed by the flocculation gene *FLO1* (YAR050) with 108 mutations and the *PRM7* (YDL039C) pheromone-regulated protein with 39 mutations (File S1). Among 90 small deletions and 60 small insertions (up to three bases) that were found in Δ8 strain, 33 were in coding regions, with the remaining 117 in noncoding regions (Table 1 and File S1). The highest number of mutations (point mutations and short indels) was observed on chromosome 7, which had 672 mutations, and the lowest on chromosome 10, which featured only 6 mutations (Figure S2A). This difference was much greater than that expected based on the difference in chromosome length (see below).

We observed a striking mutation clustering in the Δ8 strain: many mutations were in close proximity to each other, while

Table 1 Mutations observed in the original Δ8 strain compared to isogenic WT cells

	No.	Fraction
	Type of substitution	
Transition		
A:T > G:C	956	0.36
G:C > A:T	942	0.36
Transversion		
A:T > T:A	239	0.09
A:T > C:G	164	0.06
G:C > T:A	171	0.07
G:C > C:G	161	0.06
Total	2633	
	Substitutions	
Position		
Noncoding	1161	0.44
Coding	1472	0.56
Coding sequences		
Nonsense	4	0.0015
Missense	427	0.29
Silent	1041	0.71
Indels		
Noncoding	117	0.78
Coding	33	0.22

Distribution of 2633 point mutations and 150 indels identified in the initial Δ8 strain. The entire list of mutations, together with positions and nucleotide changes, is shown in File S1.

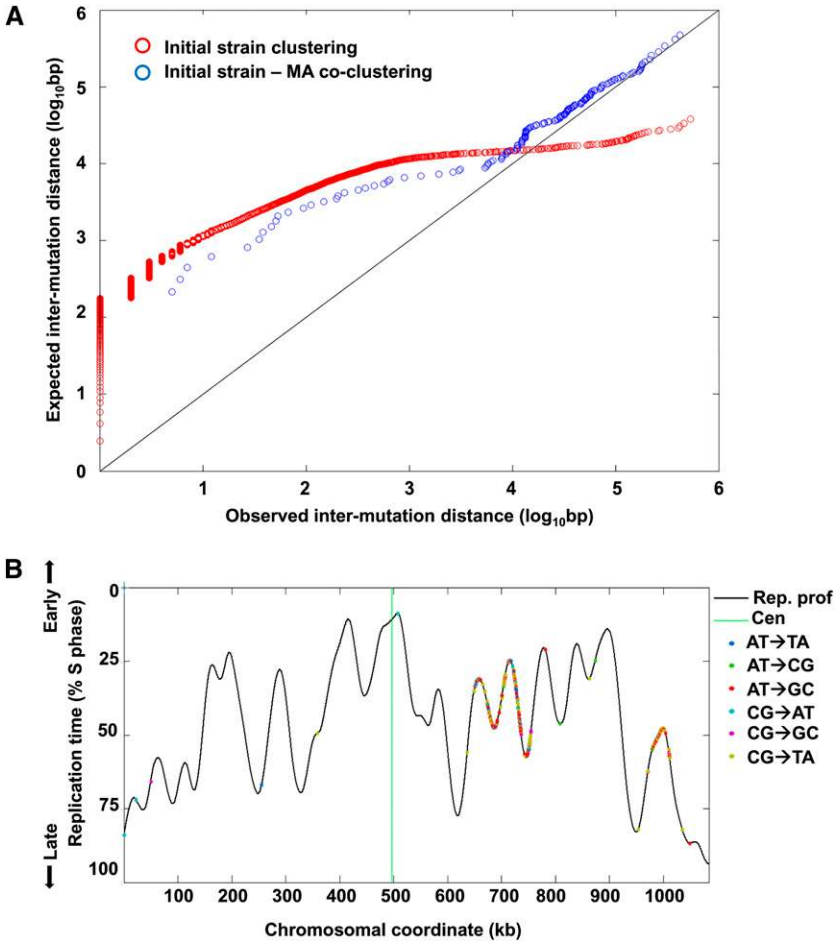

Figure 3 Mutation clustering in Δ8 cells. (A) Observed *vs.* expected distances between adjacent mutations. Observed distances are the distances between consecutive mutations on the same chromosome in the initial stain. To calculate the expected distances between mutations, we generated 100 sets of randomized genomic positions, each with the same number of loci as the number of mutations in the initial strain. We further calculated the distances between adjacent loci in each randomized set (as we did for the observed mutations) and averaged the distances across the 100 randomized iterations. Both observed and expected distances were sorted by increasing distance and plotted against each other (red circles). The diagonal represents equal expected and observed distances. As can be seen, most mutations were much closer to each other than expected by chance while mutational clusters were themselves very distant from other clusters, leading to the long tail of higher-than-expected intramutation distances. This indicates a very strong clustering of mutations along the genome. The distances between mutations in the MA lines and the nearest mutations in the initial strain were also calculated and compared to a set of 100 randomized genomic positions, each with the same number of loci as the number of mutations in the MA lines, as above. The observed *vs.* expected distances between MA line and initial strain mutations are shown in blue circles. Mutations in the MA lines tended to fall closer to initial strain mutation clusters than expected by chance. (B) An example of mutation clusters on chromosome VII of the original Δ8 strain. Shown is the DNA replication timing profile of the chromosome (black line; high values represent early replication, low values late replication; peaks correspond to replication origins and valleys to replication termini). The different mutation types are shown as dots along the replication profile. Two very tight mutation clusters can be observed (at ~640–755 kb and at ~980–1010 kb) with almost no mutations outside these two clusters. Similar plots for all chromosomes, with the locations of mutations in both the initial strain and the MA lines, are shown in Figure S2B.

individual mutation clusters were separated by long sequence stretches with almost no mutations (Figure 3A). The largest cluster occurred on chromosome 7 and extended ~150 kb. This clustering pattern was indicative of a strong mutational bias operating in this strain. Mutation clusters did not show any bias with respect to mutation spectrum; rather, they included all types of mutations, and clusters were not associated with any particular time of replication (Figure 3B and Figure S2B), nor did they correspond to the origin of replication or locations of Tys/LTRs or transfer RNAs (data not shown). However, we found that mutations tended to have repeats in closer proximity than expected (Figure S3), indicating that tandem repeat-associated mutations are a contributing factor to the genomic distribution of mutations in the initial mutant. Finally, we performed pulse-field gel electrophoresis (PFGE) to identify the large-scale genome rearrangements. PFGE revealed no apparent changes in chromosome size of the Δ8 strain compared to WT cells (Figure S4).

Decreased fitness of MA thiol peroxidase null cells

The large number of mutations observed in Δ8 cells offered an opportunity to use this strain to examine the process of MA and the relationship between mutation accumulation and cell fitness. Thus, we subjected the Δ8 strain to a year-long MA experiment, in which several separate MA lines, derived from the same culture of Δ8 cells (Δ8 initial cells), were cultured in parallel with several lines of the isogenic WT strain (also derived from the same WT culture and designated WT initial cells), each passing through 50 (once per week) single-cell bottleneck selections (Figure 4). Each bottleneck step consisted of a 3-day growth of single colonies in liquid culture followed by 4 days colonial growth on YPD agar plates. We calculated the total number of divisions as 1500 for WT and 800 for Δ8 cells. The experiment was initiated with six lines of Δ8 and three lines of WT cells. After 100 generations, one of Δ8 lines was divided into two parallel lines and named MA line 2A and 2B, thereby resulting in a total of 7 Δ8 lines.

To assess how the long-term MA experiment affected cell fitness, we compared life span and growth rate of initial and MA lines after the long-term growth of WT and Δ8 cells. Interestingly, both replicative life span and growth rate were decreased in all independent Δ8 MA lines (at least in two lines, $P < 0.05$), while this effect was not observed in WT MA lines (Figure 5). However, there was no correlation between the observed number of mutations in each line

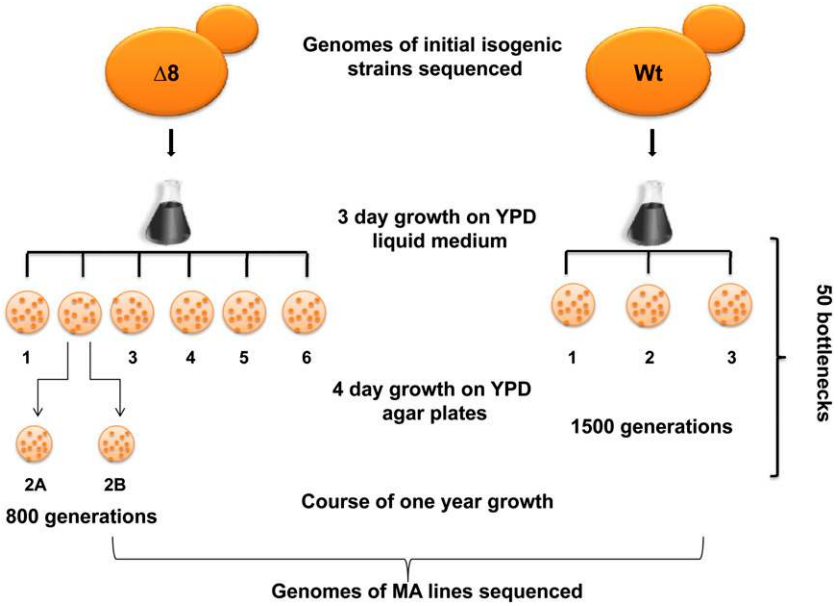

Figure 4 Experimental design of the mutation accumulation experiment. The Δ8 strain was obtained by mating Δ3 and Δ5 cells, followed by deletion of the remaining peroxidase gene (Gpx2). The genomes of initial WT and Δ8 cells were sequenced, and cells (seven MA lines for Δ8 and three MA lines for WT cells) were subjected to a bottleneck process: colonies were grown for 4 days from an individual cell on solid media followed by growth for 3 days in liquid culture. This process was repeated 50 times over the course of 1 year, followed by genome sequencing of final cell populations. One of Δ8 lines was split into two lines following 100 generations, after which they were treated as independent MA lines.

and the degree to which life span and growth rate were decreased. For example, the mutant MA line 3 accumulated 36 mutations (both point mutations and indels) and its mean replicative life span was six divisions, whereas the mutant MA line 1 had 12 mutations with the mean replicative life span of four divisions (Figure 5 and Table S2).

Thiol peroxidase null MA lines exhibit high point mutation and indel rates

We analyzed mutation rates and spectra of yeast cells by sequencing the genomes of initial strains and Δ8 and WT lines subjected to the MA procedure. A total of 132 point mutations were observed in Δ8 MA lines, but only 7 point mutations in WT MA lines. Among the 132 mutations, 49 were in noncoding regions and 83 in coding sequences, including 52 missense, 3 nonsense, and 28 silent mutations (Table 2 and Figure S5A). We identified 5 common mutations between MA lines 2A and 2B (which were separated from the common line 2 after 100 generations) and confirmed that all 5 mutations appeared prior to the separation of lines by sequencing the PCR-amplified fragments from mutated regions. The remaining 9 mutations for MA line 2A and 15 mutations for MA line 2B occurred independently and showed no overlap. The data suggest that the occurrence of 5 mutations did not drive common mutations during the rest of the experiment. No overlaps in mutations were observed among other MA lines. Mutations showed a tendency to occur in proximity to the mutation clusters in the Δ8 initial strain and co-clustering was still significantly stronger than expected by chance (Figure 3A). The overall transition rate was twofold higher than the transversion rate (Ts/Tv). The specific mutation distribution for MA lines was very similar to that of the Δ8 initial strain, but the CG→AT transversion rate was higher during the long-term growth (Figure 6A). The observed mutational pattern suggested that oxidative DNA damage had a major role. Oxidative deamination of cytosine, which leads to thymine substitution, and the high oxidation potential of guanine to 8-oxoguanine that is mismatched to adenine were in agreement with our observations (Ossowski *et al.* 2010; Thiviyanathan *et al.* 2008).

Among the seven point mutations identified in WT MA lines, four were in coding regions and three in untranslated regions (Table 2 and Figure S6A). The average base substitution rate was 15-fold higher in Δ8 MA lines (19.9×10^{-10} per site per generation for Δ8 MA lines and 1.3×10^{-10} for WT lines). We also calculated the MA line-specific base substitution mutation rates for each Δ8 line, which varied from 9.59×10^{-10} to 28.6×10^{-10} (Figure 6B).

The genomes of MA lines were further analyzed to identify small indels of 1–3 bp, identifying 17 insertions and 18 deletions in Δ8 MA lines. The majority of indels were in noncoding areas, with six occurring in coding regions. Of 29 intergenic indels, 10 were found in telomeric regions (Table 2 and Figure S5, B and C). We also identified 3 single-base-pair deletions in the mitochondrial genome of three MA lines. As mentioned above, there were substitutions and small indels identified in the mitochondrial genome of the initial Δ8 strain, and several more accumulated during the long-term growth of the MA lines. However, mitochondria were still functional in all Δ8 MA lines at the end of the 1-year growth, indicating that the observed mutations did not interfere with the respiratory function in any of the MA lines (Figure S1). Further analysis of the genomes of WT MA lines revealed a total of 5 small insertions, including 3 in coding regions, whereas we did not detect small deletions (Table 2 and Figure S6B). Only one WT line harbored a single double-nucleotide insertion in the mitochondrial genome, which also occurred in the noncoding region. We did not observe mutational hotspots during the long-term growth of WT or Δ8 MA lines. The average rates of short indels were estimated at 5.3×10^{-10} for Δ8 and 0.94×10^{-10} for WT lines, and the individual indel mutation rates varied from 2.1×10^{-10}

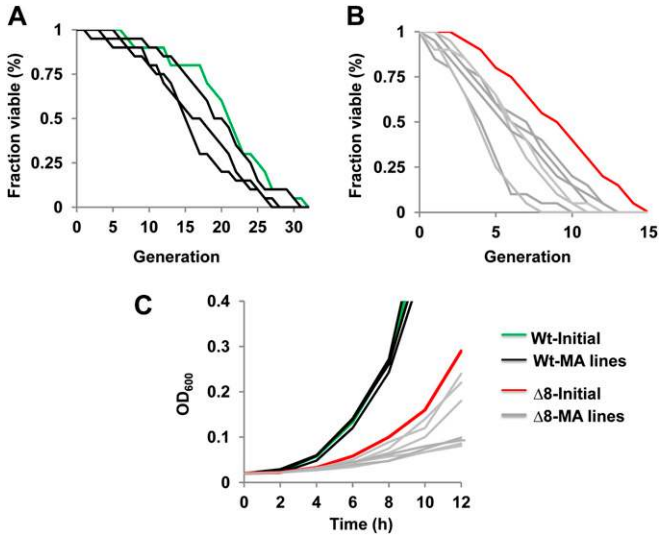

Figure 5 Decreased fitness of MA lines. Twenty individual virgin daughter cells were collected for corresponding WT and Δ8 MA lines and analyzed by using a microscope with a micromanipulator to determine replicative life span. Statistical analysis of the life-span data were performed using a Wilcoxon rank-sum test. *P*-value data for this experiment are in Table S2. (A) Replicative life span of WT initial (green line) and WT MA lines (black lines). (B) Replicative life span of Δ8 initial (red line) and Δ8 MA lines (gray lines). (C) Growth rate of initial and MA Δ8 lines.

to 10.6×10^{-10} per site per generation in Δ8 MA lines (Figure 6B and Table 2).

Characterization of an independent Δ8 isolate

Genome instability was a striking phenotype of the Δ8 mutant, but a possibility remained that this mutator phenotype was the result of a single mutational catastrophe during preparation of the Δ8 mutant rather than the result of thiol peroxidase deficiency. To address this possibility, we prepared an independent Δ8 isolate from Δ3 and Δ5 cells, this time with a minimal number of generations, and further sequenced the genome of this strain. The new mutant also had a very strong mutator phenotype. We detected 230 point mutations and 15 small indels in this mutant, which corresponded to ~2 mutations per generation during strain construction; this can be compared with the observed 2.2 mutations per 1500 generations in WT cells (Figure 7 and File S1). We characterized several phenotypes of this new mutant and found its overall behavior was similar to that of the original Δ8 strain, including reduced growth rate and shortened replicative life span (Figure 1). The mutation spectrum of the new isolate was also similar to that of the previous isolate, and CG→TA transitions were much more common than other mutation types (Figure 7D). There were 20 commonly mutated genes, with the majority of these genes inherited from the Δ5 cells during the mating process. These mutated genes featured nucleotide substitution mutations except for the metallochaperone Mtm1, which had a frameshift in the first isolate and a substitution mutation in the second isolate. It is difficult to evaluate the functional consequences of mutated genes, if any, for the observed phenotypes (File S1).

Table 2 Mutations observed in WT and Δ8 MA lines following the long-term MA experiment

	WT			Δ8						
Substitutions	1	2	3	1	2A	2B	3	4	5	6
Position										
Noncoding	1	0	0	4	7	10	8	6	4	10
Nonsense	0	0	0	1	1	0	0	0	0	1
Missense	1	0	2	2	2	6	14	8	10	10
Silent	0	2	1	2	4	4	6	8	0	4
Indels										
Position										
Noncoding	1	1	0	3	3	9	7	4	2	1
Coding	2	0	1	0	1	1	1	1	0	2
All mutations	5	3	4	12	18	30	36	27	16	28
Mutation rate ($\times 10^{-10}$)	2.8	1.7	2.2	12.7	19	31.8	37.1	29.6	16.9	29.6
Mean ($\times 10^{-10}$)		2.2					25.3			

Mutation distributions for each MA line are shown. Mutation rates were calculated based on the total number of substitutions and small indels per site per generation. The entire list of mutations together with positions and nucleotide changes is shown in Figure S5 and Figure S6.

An additional consistent observation with the new isolate was that mutations tended to be in close proximity to each other (Figure S7). Overall, these data showed that deficiency in eight thiol peroxidases leads to a strong mutator phenotype in yeast cells, characterized by point mutations and indels and pointing to a critical role of these proteins in genome stability.

Deletion of eight thiol peroxidases modulates sensitivity of cells to DNA damage

To test whether the impaired proliferation and the observed mutator phenotype of Δ8 cells were related to DNA replication and repair, we examined the sensitivity of cells to genotoxic stresses. Cells were treated with camptothecin and hydroxyurea, which are commonly used as replication inhibitors, and with benomyl, which affects the function of microtubules, causing improper chromosome segregation during cell division and delayed DNA replication (van Loon *et al.* 2010; Sheltzer *et al.* 2011). In addition, we treated cells with phelomycin, which induces double-strand breaks that are repaired by homologous recombination (Reiter *et al.* 1972). In all cases, the Δ5Prxs and Δ8 strains, but not the Δ3Gpxs strain, displayed significant sensitivity to these drugs, suggesting that the observed slow proliferation phenotype could be related to the defect in both replication and recombinational repair processes in the absence of peroxiredoxins (Figure 8A). Consistent with this observation, the new Δ8 isolate showed the same sensitivity to all these drugs (Figure S8). It is known that in most cancer types replication stress causes an aggressive mutator phenotype (Loeb 2001). These observations support the idea that thiol peroxidases have critical roles in the DNA damage response and in ROS control. Accordingly, deficiency in these enzymes leads to a strong mutator phenotype by delaying replication.

Consistent transcriptome landscape of Δ8 cells

Even though there was a 10-fold difference in mutations and a large difference in the number cell divisions between the

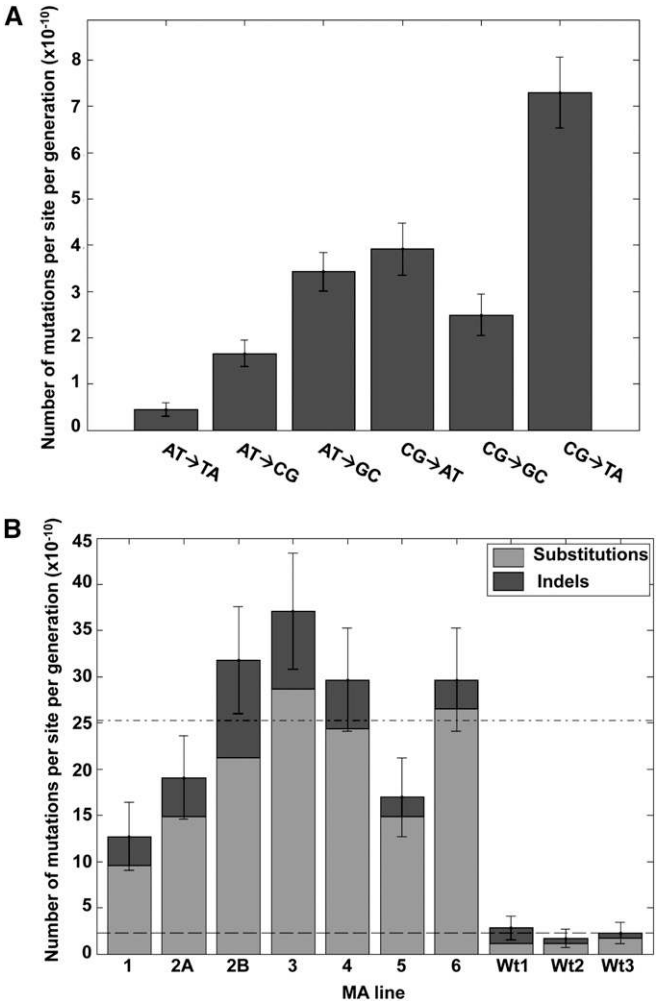

Figure 6 Observed mutation rates for MA lines. (A) Observed total mutation rates per site/per generation after the long-term growth of MA lines. Shown is the average for all MA lines. (B) The mutation rate and standard error per MA line. Horizontal dashed lines are the average mutation rate (base substitutions and indels) for the Δ8 and the WT lines.

two Δ8 strains, both independent isolates were similar with regard to growth characteristics, drug sensitivity, and life span, suggesting that the observed phenotypic changes were largely due to thiol peroxidase deficiency. We further examined this possibility by analyzing gene expression via RNA-seq. The numerous mutations that independently emerged in two Δ8 mutant strains did not result in significant differences in their gene expression, as the expression of 4493 genes was highly correlated ($\rho = 0.97$) (Figure 8A and File S2). At the same time, the expression of 90% genes varied between −0.73 and 0.99 (Log2) in both Δ8 isolates, and 10% of genes increased or decreased expression at least twofold, compared to WT cells (Figure 8A). We were particularly interested in the transcriptional regulation of DNA repair genes as it could provide further molecular insights into the basis for the mutator phenotype of Δ8 cells. A total of 183 such genes are known to maintain stability of the yeast nuclear genome (File S2). We found that the expression of these genes was well correlated ($\rho = 0.99$), and most of them were upregulated in both Δ8 isolates compared to WT cells (Figure 8B). Among these genes, ubiquitin-dependent DNA repair genes, which are involved in the nonhomologous end-joining pathway that repairs double-strand breaks, were top hits. Recently, it was shown that this pathway promotes DNA repair, supporting cell survival following DNA repair (Kato *et al.* 2014). Perhaps, the error-prone double-strand break repair in the repetitive regions initiates mutations in Δ8 cells, leading to the observed clustered mutation pattern.

Overexpression of the abundant thiol peroxidase Tsa1 partially restores the growth phenotype

To further characterize the consequences of deleting eight thiol peroxidase genes, we tested the complementation of growth of mutant cells by overexpressing Tsa1 under the constitutive yeast *TEF1* promoter. Tsa1 was previously described as a highly abundant peroxidase that suppresses genome instability (Iraqui *et al.* 2009). In WT cells, its expression did not affect cell growth. The slow growth of thiol peroxidase null strains was partially restored in the logarithmic phase by Tsa1 expression, but both populations attained a lower level of cell density than either WT or control Δ8 cells (Figure 9A). Thus, expression of Tsa1 only partially rescued the growth of Δ8 cells. We also confirmed the restoration of growth by spotting equal amounts of cells onto YPD plates and examining them 3 days later (Figure 9B).

Discussion

It has been ∼2.5 billion years since the great oxygenation event (GOE). The cost of living in an oxygen-rich environment is currently the subject of intense research. Evidence indicates that, in addition to evolving ways to utilize O_2, organisms developed defense systems against dangers posed by ROS and oxidative stress in general. Thiol peroxidases are the enzymes that clear low levels of hydroperoxides from cells, but they may differ from other antioxidant proteins since they are also found in anaerobes. In fact, they occur in nearly every living organism, indicating that they evolved prior to the GOE (Edgar *et al.* 2012). Thus, additional, presumably more ancient, noncanonical roles of peroxidases might not be known.

In the current study, we performed whole-genome sequencing to characterize the impact of thiol peroxidase deficiency on genome stability, following the deletion of all Prxs (five genes) and Gpxs (three genes). These Δ8 cells were viable, but manifested several phenotypes indicative of decreased fitness, such as slow growth, shorter life span, and decreased colony size in two independent Δ8 isolates. We cannot completely exclude the possibility that some of these phenotypes were affected by nonperoxidase mutations, but the striking similarity between the two independent preparations of Δ8 mutants, which did not share common mutations, argues against this possibility. It should be noted, however, that, because it is difficult to generate a clean (isogenic to wild type) Δ8 strain, nonperoxidase mutations may play some

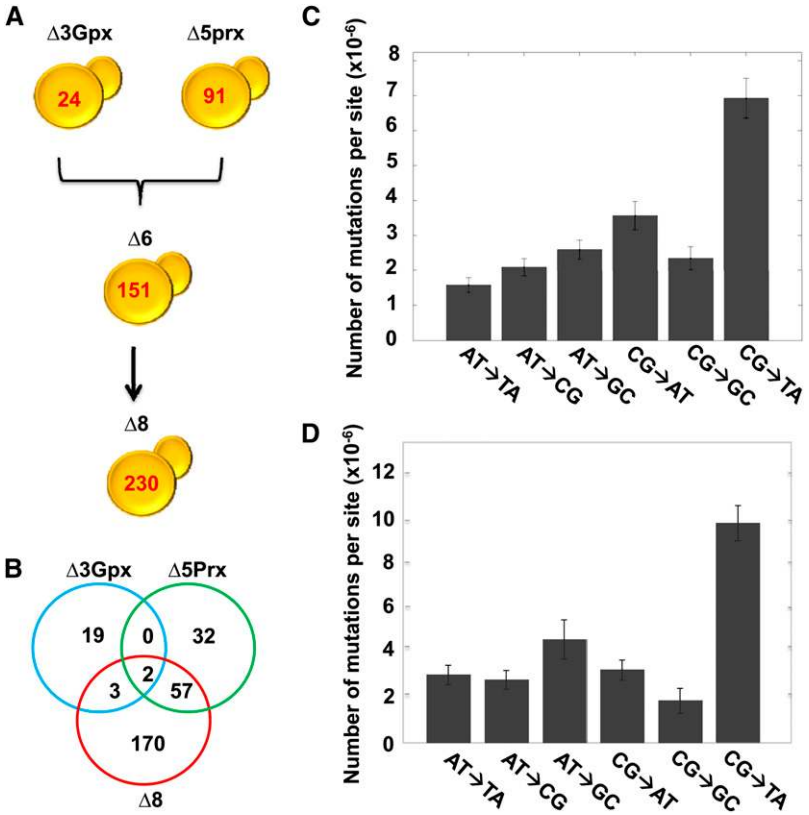

Figure 7 Characterization of mutations in an independent Δ8 isolate. (A–C) Quantification of mutations and characterization of the second Δ8 mutant are as shown in Figure 2 for the first Δ8 mutant. (D) Mutations found in Δ7 were subtracted from the first Δ8 mutant strain, and the spectrum of remaining mutations was analyzed.

role. Regardless, our key finding was that both isolates had a very strong mutator phenotype, leading to the accumulation of numerous mutations in their genomes that were different in the two Δ8 mutants and suggesting that it is the absence of thiol peroxidases that compromises genome integrity.

To further address the role of thiol peroxidases in genome stability, we designed a controlled experiment, wherein WT (three independent lines) and Δ8 cells (seven independent lines) were subjected to a parallel, long-term MA experiment, characterized by 50 weekly bottlenecks. After this long-term growth, we compared the replicative life span and growth characteristics for all experimental MA lines. Interestingly, there was a reduction in fitness in all Δ8 MA lines for both life span and growth rate. This experiment showed that all seven parallel Δ8 MA lines became increasingly vulnerable during growth in the absence of thiol peroxidases. Since thiol peroxidases are highly conserved proteins and occur in nearly all living organisms, these results suggest that the presence of these enzymes is required for protection and recovery of populations from natural collapse, subject to environmental and genetic challenges.

We sequenced the genomes of initial and MA Δ8 and WT strains and compared their mutation spectra. All Δ8 lines had significantly more mutations than any of the WT lines: the average mutation rate (base substitutions and indels) of the mutant MA lines was 11-fold higher than that of the WT MA lines. We observed 0.0027 mutations per generation (12 mutations/three lines/1500 generations) for WT and 0.03 mutations per generation (167 mutations/seven lines/800 generations) for the Δ8 mutant. The mutation rate for WT was consistent with a previous measurement (Lynch *et al.* 2008). The variation among mutation rates for each MA line could be an indicator of the influence of new mutations. There were almost 200 genes having missense and/or frameshift mutations in the initial Δ8 strain, which possibly interfered with the function of these proteins, including some DNA repair enzymes, thereby affecting the mutation rate. This issue highlights the difficulty in determining a single mutation rate as it changes over time.

We did not identify recurrent mutations among MA lines. One interesting observation in the Δ8 strains was the finding of long clusters of mutations. Proximity of these mutations suggested that clustered events could reduce the deleterious effects of random mutations or that mutations in the regions that harbor nonessential genes are preserved and enriched, while mutations in more critical regions lead to lethality and so could not be recovered in our bottleneck selection design. A similar mutation clustering was recently reported in another yeast experiment (Roberts *et al.* 2012). This study observed nonrandom biased clustered mutations near chromosome breakpoints, which had a common motif targeted by specific deaminases. Our results also indicate that there could be a different intrinsic mechanism for the observed mutation distribution in the thiol peroxidase null strain in parallel to random selection, resulting in such an extensive mutation pattern.

To test for general association of mutations in the initial strain and tandem repeats, we analyzed the distribution of distances between mutations and repeats, comparing them

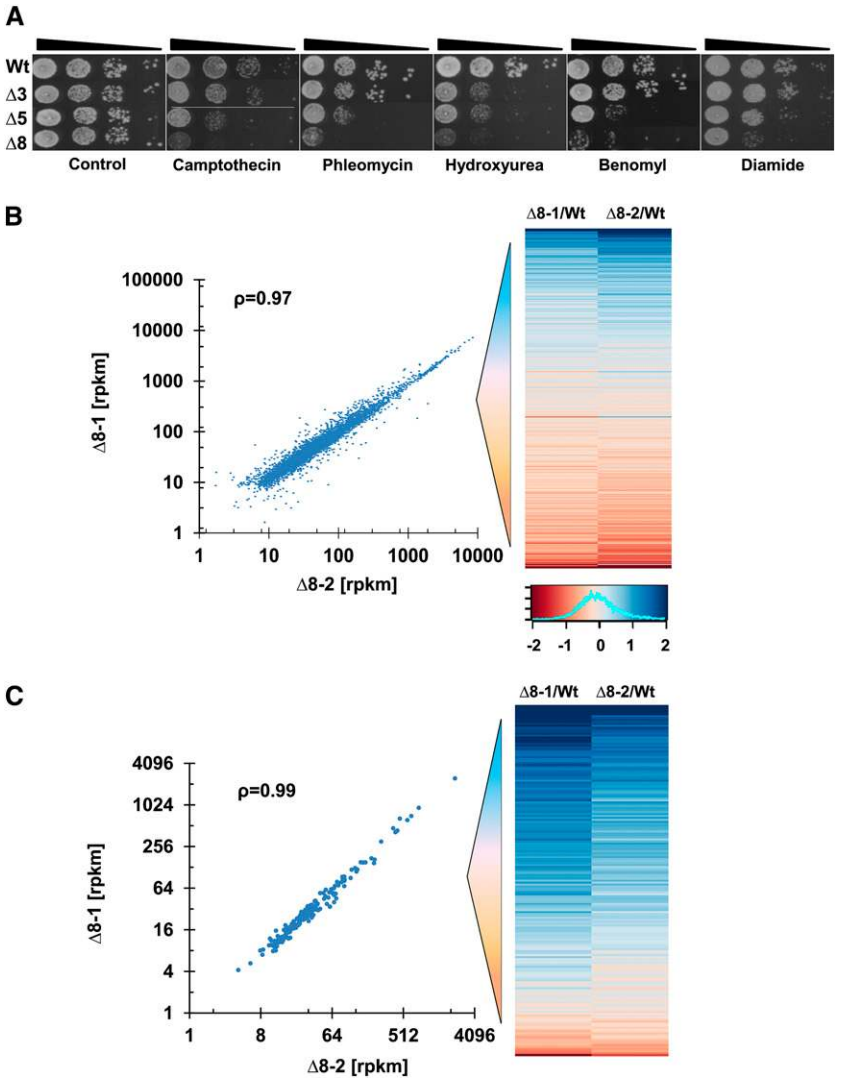

Figure 8 Spot assay and comparison of gene expression data. (A) Sensitivity of Δ8 and WT cells to DNA damage agents. In the control panel, Δ8 and Δ5 cells were used with a twofold higher cell density compared to other strains to observe similar growth. Ten-fold dilution of WT and Δ8 cells grown on YPD plates containing 15 μg/ml camptothecin (replication inhibitor), 150 mM hydroxyurea (replication inhibitor), 0.3 μg/ml phleomycine (double-strand break inducer), or 15 μg/ml benomyl (microtubule poison). (B) Comparison of expression of 4493 genes in Δ8 isolates with the expression graded as log2 of the fold increase/decrease in the heat map on the right, ranked from high (blue) to low (red). Mean rpkm (reads per kilobase transcript per million reads) values of two repetitions for each Δ8 isolate were calculated, the values <10 in both isolates were eliminated, and Spearman correlation (ρ) was calculated. Expression distribution of genes for both Δ8 isolates is shown by a histogram at the bottom right. (C) Analysis of genes known to regulate stability of the nuclear genome.

to the distances expected by chance (Figure 3 and Figure S3). It is known that these repetitive DNA sequences are highly unstable and mutate at high rates, including a high frequency of double-strand DNA breaks (Bzymek and Lovett 2001; Gemayel *et al.* 2010). It appears that the observed long stretches of mutation clusters in Δ8 cells could be initiated at tandem repeats initiated by double-strand DNA breaks. Subsequently, error-prone repair could introduce additional mutations in these regions. Apparently, this observation is also applicable to the second Δ8 isolate since clustering was also observed in this mutant. A second line of evidence from gene expression data also supports this hypothesis as most of the double-strand DNA break repair genes were upregulated in both Δ8 strains.

Our genotoxic assays and transcriptome analyses also suggest additional mechanisms by which thiol peroxidases may maintain genome stability. The Δ8 strains are very sensitive to replication inhibitors and microtubule poisons, which delay DNA replication and cellular proliferation, respectively. It appears that DNA damage occurs in the absence of thiol peroxidases as a consequence of oxidative stress, even if this stress is relatively mild. We hypothesize that thiol peroxidases interact with transcription factors to activate or repress gene expression. In the absence of thiol peroxidases, transcription regulation of these cells is compromised. This may be an additional factor that contributes to the high mutator phenotype in Δ8 cells. A global regulatory role of peroxidases in transcriptional signaling is consistent with this idea (Fomenko *et al.* 2011). Finally, we showed that overexpression of a major thiol peroxidase Tsa1 was able to partially rescue the growth phenotype of Δ8 cells.

We described the mutational landscape of cells lacking thiol peroxidases and showed that these enzymes have important roles in maintaining genome integrity due to counteracting the damaging effects of low levels of peroxides and regulating DNA repair genes. Our genome analyses suggested that, in the original Δ8 strain, deletion of all eight thiol peroxidase genes coincided with a rapid accumulation of many mutations (while very few mutations were detected in Δ3 and Δ5 mutants), but subsequently changes accumulated in the genome that slowed down the mutation rate (based on the mutation rate of Δ8 cells revealed by our long-term MA experiment). In the

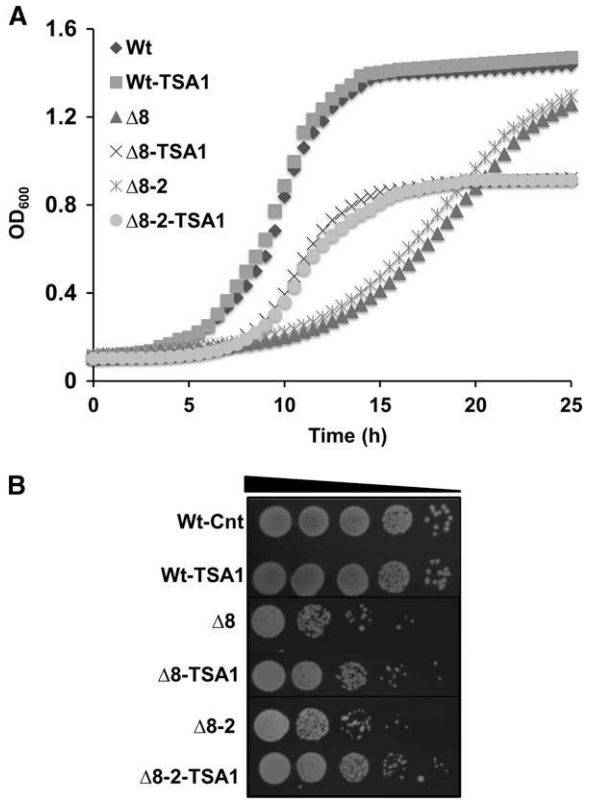

Figure 9 Expression of *TSA1* in Δ8 cells. (A) Reduced cell growth of Δ8 cells was partially rescued by Tsa1 expression. Growth of WT and Δ8 cells expressing (or not) TSA1 in liquid YPD medium containing 20 μg/ml phleomycin was monitored by measuring the OD_{600} every 30 min. Mean values of two independent measurements for each point are shown. (B) Colony growth of Tsa1-expressing Δ8 cells. Overnight cultures of WT and two independent Δ8 isolates as well as the corresponding strains expressing Tsa1 were diluted to an OD_{600} of 0.3. Then, 5 μl of 10-fold dilution of each cell suspension were spotted onto YPD plates containing 20 μg/ml and photographed 3 days later.

independent Δ8 isolate, the mutation rate was also very high, but not as high (even considering the few cell divisions). Perhaps, a mutational catastrophe occurred during meiosis that led to Δ7 cells, prior to preparation of Δ8 cells. Indeed, the number of mutations from this step to create Δ8 was similar to that observed in the second Δ8 isolate and MA lines (Figure 7D).

It was shown previously that yeast cells can withstand the rate of $\sim 10^{-3}$ mutations per gene per cell division (Herr *et al.* 2011). Above this threshold, cells eventually die, and only the cells with suppressor mutations that decrease the rate of error-prone replication escape from extinction. Such suppressors may tolerate substantial increase in mutation rate before losing viability (Herr *et al.* 2011). We speculate that the observed reduced mutation rate in Δ8 MA lines reflects the fact that these cells acquired important modifier loci to suppress the high mutation rate of the Δ8 cells. There is also evidence for a further reduction in mutation rate during strain construction: lines 2A/B had 5 mutations during the first 100 generations of the MA procedure, whereas line 2A had only 9 additional and line 2B 15 additional mutations in the remaining 700 generations (for line 2A, this is a significant reduction; Fisher's exact, $P = 0.025$). This implies that selection might have acted during the MA procedure and that the mutation rate declined, perhaps also partially affecting the spectrum of mutations. Cells with deleterious mutations were eliminated following each bottleneck, and cells with the acquired lower mutator phenotype were selected. In the end, we observed lower-than-expected (based on the comparison of WT and Δ8 genomes) numbers of mutations in MA lines following the long-term growth experiment, although these numbers were still much higher than mutations in the WT MA cells.

We presented the first genome-wide mutation spectrum of cells as a consequence of thiol peroxidase deficiency, which uncovered an important function of these enzymes in genome stability. There are several reports showing that mice lacking Prdx1, an ortholog of yeast Tsa1p, are highly prone to the development of various malignancies (Neumann *et al.* 2003; Egler *et al.* 2005). Our study supports the idea that thiol peroxidases are key protectors against DNA damage and genome instability and can serve as tumor suppressors under conditions of oxidative stress. These genes are conserved in all three domains of life and are present in nearly all living organisms, but often they are not essential when knocked out in various organisms. Understanding the mechanism by which they contribute to genome stability offers insights into their functions, conservation in the three domains of life, and essential roles in DNA maintenance and protection against cancer.

Acknowledgments

We thank Shamil Sunyaev and Paz Polak for discussion and Siming Ma for help with RNAseq data analysis. This work was supported by National Institutes of Health grant GM065204 to V.N.G.

Literature Cited

Avery, A. M., and S. V. Avery, 2001 Saccharomyces cerevisiae expresses three phospholipid hydroperoxide glutathione peroxidases. J. Biol. Chem. 276: 33730–33735.

Brigelius-Flohe, R., 1999 Tissue-specific functions of individual glutathione peroxidases. Free Radic. Biol. Med. 27: 951–965.

Brigelius-Flohe, R., 2006 Glutathione peroxidases and redox-regulated transcription factors. Biol. Chem. 387: 1329–1335.

Bzymek, M., and S. T. Lovett, 2001 Instability of repetitive DNA sequences: the role of replication in multiple mechanisms. Proc. Natl. Acad. Sci. USA 98: 8319–8325.

Cooke, M. S., M. D. Evans, M. Dizdaroglu, and J. Lunec, 2003 Oxidative DNA damage: mechanisms, mutation, and disease. FASEB J. 17: 1195–1214.

Degtyareva, N. P., L. Chen, P. Mieczkowski, T. D. Petes, and P. W. Doetsch, 2008 Chronic oxidative DNA damage due to DNA repair defects causes chromosomal instability in Saccharomyces cerevisiae. Mol. Cell. Biol. 28: 5432–5445.

Denver, D. R., K. Morris, M. Lynch, and W. K. Thomas, 2004 High mutation rate and predominance of insertions in the Caenorhabditis elegans nuclear genome. Nature 430: 679–682.

Edgar, R. S., E. W. Green, Y. Zhao, G. van Ooijen, M. Olmedo *et al.*, 2012 Peroxiredoxins are conserved markers of circadian rhythms. Nature 485: 459–464.

Egler, R. A., E. Fernandes, K. Rothermund, S. Sereika, N. de Souza-Pinto *et al.*, 2005 Regulation of reactive oxygen species, DNA damage, and c-myc function by peroxiredoxin 1. Oncogene 24: 8038–8050.

Fomenko, D. E., A. Koc, N. Agisheva, M. Jacobsen, A. Kaya *et al.*, 2011 Thiol peroxidases mediate specific genome-wide regulation of gene expression in response to hydrogen peroxide. Proc. Natl. Acad. Sci. USA 108: 2729–2734.

Gemayel, R., M. D. Vinces, M. Legendre, and K. J. Verstrepen, 2010 Variable tandem repeats accelerate evolution of coding and regulatory sequences. Annu. Rev. Genet. 44: 445–477.

Gerashchenko, M. V., A. V. Lobanov, and V. N. Gladyshev, 2012 Genome-wide ribosome profiling reveals complex translational regulation in response to oxidative stress. Proc. Natl. Acad. Sci. USA 109: 17394–17399.

Herr, A. J., M. Ogawa, N. A. Lawrence, L. N. Williams, J. M. Eggington *et al.*, 2011 Mutator suppression and escape from replication error-induced extinction in yeast. PLoS Genet. 7: e1002282.

Horling, F., P. Lamkemeyer, J. Konig, I. Finkemeier, A. Kandlbinder *et al.*, 2003 Divergent light-, ascorbate-, and oxidative stress-dependent regulation of expression of the peroxiredoxin gene family in Arabidopsis. Plant Physiol. 131: 317–325.

Huang, M. E., A. G. Rio, A. Nicolas, and R. D. Kolodner, 2003 A genomewide screen in Saccharomyces cerevisiae for genes that suppress the accumulation of mutations. Proc. Natl. Acad. Sci. USA 100: 11529–11534.

Inoue, Y., T. Matsuda, K. Sugiyama, S. Izawa, and A. Kimura, 1999 Genetic analysis of glutathione peroxidase in oxidative stress response of Saccharomyces cerevisiae. J. Biol. Chem. 274: 27002–27009.

Iraqui, I., G. Kienda, J. Soeur, G. Faye, G. Baldacci *et al.*, 2009 Peroxiredoxin Tsa1 is the key peroxidase suppressing genome instability and protecting against cell death in Saccharomyces cerevisiae. PLoS Genet. 5: e1000524.

Kato, K., K. Nakajima, A. Ui, Y. Muto-Terao, H. Ogiwara *et al.*, 2014 Fine-tuning of DNA damage-dependent ubiquitination by OTUB2 supports the DNA repair pathway choice. Mol. Cell 53: 617–630.

Kryston, T. B., A. B. Georgiev, P. Pissis, and A. G. Georgakilas, 2011 Role of oxidative stress and DNA damage in human carcinogenesis. Mutat. Res. 711: 193–201.

Li, H., and R. Durbin, 2009 Fast and accurate short read alignment with burrows-wheeler transform. Bioinformatics 25: 1754–1760.

Loeb, L. A., 2001 A mutator phenotype in cancer. Cancer Res. 61: 3230–3239.

Lynch, M., W. Sung, K. Morris, N. Coffey, C. R. Landry *et al.*, 2008 A genome-wide view of the spectrum of spontaneous mutations in yeast. Proc. Natl. Acad. Sci. USA 105: 9272–9277.

Marnett, L. J., 2000 Oxyradicals and DNA damage. Carcinogenesis 21: 361–370.

McKenna, A., M. Hanna, E. Banks, A. Sivachenko, K. Cibulskis *et al.*, 2010 The genome analysis toolkit: a MapReduce framework for analyzing next-generation DNA sequencing data. Genome Res. 20: 1297–1303.

Michaelson, J. J., Y. Shi, M. Gujral, H. Zheng, D. Malhotra *et al.*, 2012 Whole-genome sequencing in autism identifies hot spots for de novo germline mutation. Cell 151: 1431–1442.

Milne, I., M. Bayer, L. Cardle, P. Shaw, G. Stephen *et al.*, 2010 Tablet: next generation sequence assembly visualization. Bioinformatics 26: 401–402.

Muller, F. L., M. S. Lustgarten, Y. Jang, A. Richardson, and H. Van Remmen, 2007 Trends in oxidative aging theories. Free Radic. Biol. Med. 43: 477–503.

Neumann, C. A., D. S. Krause, C. V. Carman, S. Das, D. P. Dubey *et al.*, 2003 Essential role for the peroxiredoxin Prdx1 in erythrocyte antioxidant defence and tumour suppression. Nature 424: 561–565.

Nishant, K. T., W. Wei, E. Mancera, J. L. Argueso, A. Schlattl *et al.*, 2010 The baker's yeast diploid genome is remarkably stable in vegetative growth and meiosis. PLoS Genet. 6: e1001109.

Ossowski, S., K. Schneeberger, J. I. Lucas-Lledo, N. Warthmann, R. M. Clark *et al.*, 2010 The rate and molecular spectrum of spontaneous mutations in Arabidopsis thaliana. Science 327: 92–94.

Park, S. G., M. K. Cha, W. Jeong, and I. H. Kim, 2000 Distinct physiological functions of thiol peroxidase isoenzymes in Saccharomyces cerevisiae. J. Biol. Chem. 275: 5723–5732.

Reddy, V. P., X. Zhu, G. Perry, and M. A. Smith, 2009 Oxidative stress in diabetes and Alzheimer's disease. J. Alzheimers Dis. 16: 763–774.

Reiter, H., M. Milewskiy, and P. Kelley, 1972 Mode of action of phleomycin on Bacillus subtilis. J. Bacteriol. 111: 586–592.

Rhee, S. G., H. Z. Chae, and K. Kim, 2005 Peroxiredoxins: a historical overview and speculative preview of novel mechanisms and emerging concepts in cell signaling. Free Radic. Biol. Med. 38: 1543–1552.

Roberts, S. A., J. Sterling, C. Thompson, S. Harris, D. Mav *et al.*, 2012 Clustered mutations in yeast and in human cancers can arise from damaged long single-strand DNA regions. Mol. Cell 46: 424–435.

Schneeberger, K., J. Hagmann, S. Ossowski, N. Warthmann, S. Gesing *et al*, 2009 Simultaneous alignment of short reads against multiple genomes. Genome Biol. 10: R98.

Sheltzer, J. M., H. M. Blank, S. J. Pfau, Y. Tange, B. M. George *et al.*, 2011 Aneuploidy drives genomic instability in yeast. Science 333: 1026–1030.

Tang, H. M., K. L. Siu, C. M. Wong, and D. Y. Jin, 2009 Loss of yeast peroxiredoxin Tsa1p induces genome instability through activation of the DNA damage checkpoint and elevation of dNTP levels. PLoS Genet. 5: e1000697.

Thiviyanathan, V., A. Somasunderam, D. E. Volk, T. K. Hazra, S. Mitra *et al.*, 2008 Base-pairing properties of the oxidized cytosine derivative, 5-hydroxy uracil. Biochem. Biophys. Res. Commun. 366: 752–757.

van Loon, B., E. Markkanen, and U. Hubscher, 2010 Oxygen as a friend and enemy: how to combat the mutational potential of 8-oxo-guanine. DNA Repair (Amst.) 9: 604–616.

Vickers, C. E., S. F. Bydder, and L. K. Nielsen, 2013 Dual gene expression cassette vectors with antibiotic selection markers for engineering in Saccharomyces cerevisiae. Microb. Cell Fact. 12: 96.

Wong, C. M., Y. Zhou, R. W. Ng, H. F. Kung Hf, and D. Y. Jin, 2002 Cooperation of yeast peroxiredoxins Tsa1p and Tsa2p in the cellular defense against oxidative and nitrosative stress. J. Biol. Chem. 277: 5385–5394.

Wong, C. M., K. L. Siu, and D. Y. Jin, 2004 Peroxiredoxin-null yeast cells are hypersensitive to oxidative stress and are genomically unstable. J. Biol. Chem. 279: 23207–23213.

Communicating editor: J. A. Nickoloff

GENETICS

Supporting Information
http://www.genetics.org/lookup/suppl/doi:10.1534/genetics.114.169243/-/DC1

Thiol Peroxidase Deficiency Leads to Increased Mutational Load and Decreased Fitness in *Saccharomyces cerevisiae*

Alaattin Kaya, Alexei V. Lobanov, Maxim V. Gerashchenko, Amnon Koren, Dmitri E. Fomenko, Ahmet Koc, and Vadim N. Gladyshev

DOI: 10.1534/genetics.114.169243

Figure S1

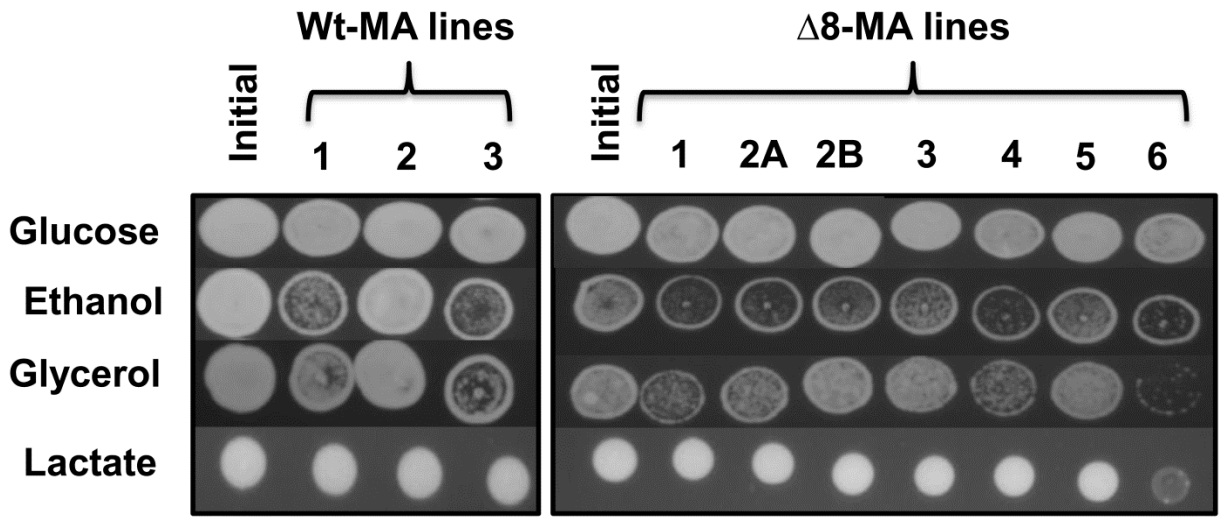

Figure S1. Spotting assay using respiratory substrates for initial and all MA lines. Wt and Δ8 strains were analyzed on plates containing 2% glucose (Glu), ethanol (EtOH), glycerol (Gly) and lactic acid (Lac), respectively, to analyze the function of mitochondria. Left panel shows the growth of Wt lines and right panel of Δ8 lines. All MA lines were able to utilize all respiratory substrates excluding the Δ8 MA line 6, which showed poor growth on glycerol and lactic acid plates.

Table S1. Yeast strains used in this study.

Strain	Designation of Wt and mutant cells	Genotype	Source
BY4741	Wt	MAT a *his3 leu2 met15 ura3*	ATCC
GY25	Δ3Gpx	MAT a *his3 leu2 met15 ura3* Δ*gpx1:URA3,* Δ*gpx2:HIS3,* Δ*gpx3: KAN*	Avery et al., 2001
GY14	Δ5Prx	MATa *his3 leu2 met15 ura3* Δ*tsa1:KAN,* Δ*tsa2:LEU2,* Δ*dot5:MET15,* Δ*ahp1:HIS3,* Δ*prx1:URA3*	Wong et al., 2004
GY150	Δ6 (all ΔPrx +ΔGpx1)	MATa *his3 leu2 met15 ura3* Δ*gpx3:KAN, URA3,* Δ*tsa1:KAN,* Δ*tsa2:LEU2,* Δ*dot5:MET15,* Δ*ahp1:HIS3,* Δ*prx1:URA3*	This study
GY29	Δ7 (all ΔPrx+2 ΔGpx1,3)	MATa *his3 leu2 met15 ura3* Δ*gpx1:URA3,* Δ*gpx3:KAN,* Δ*tsa1:KAN,* Δ*tsa2:LEU2,* Δ*dot5:MET15,* Δ*ahp1:HIS3,* Δ*prx1:URA3*	Fomenko et al., 2011
GY100	Δ8 (all ΔPrx+all ΔGpx)	MATa *his3 leu2 met15 ura3* Δ*tsa1:KAN,* Δ*tsa2:LEU2,*Δ*dot5:MET15,* Δ*ahp1:HIS3,* Δ*prx1:URA3,* Δ*gpx2:HYG,* Δ*gpx1:URA3,* *Δgpx3:KAN*	Fomenko et al., 2011
GY151	Δ8 (all ΔPrx+all ΔGpx)	MATa *his3 leu2 met15 ura3* Δ*tsa1:KAN,* Δ*tsa2:LEU2,*Δ*dot5:MET15,* Δ*ahp1:HIS3,* Δ*prx1:URA3,* Δ*gpx2:HYG,* Δ*gpx1:NAT,* *Δgpx3:KAN*	This study

Figure S2

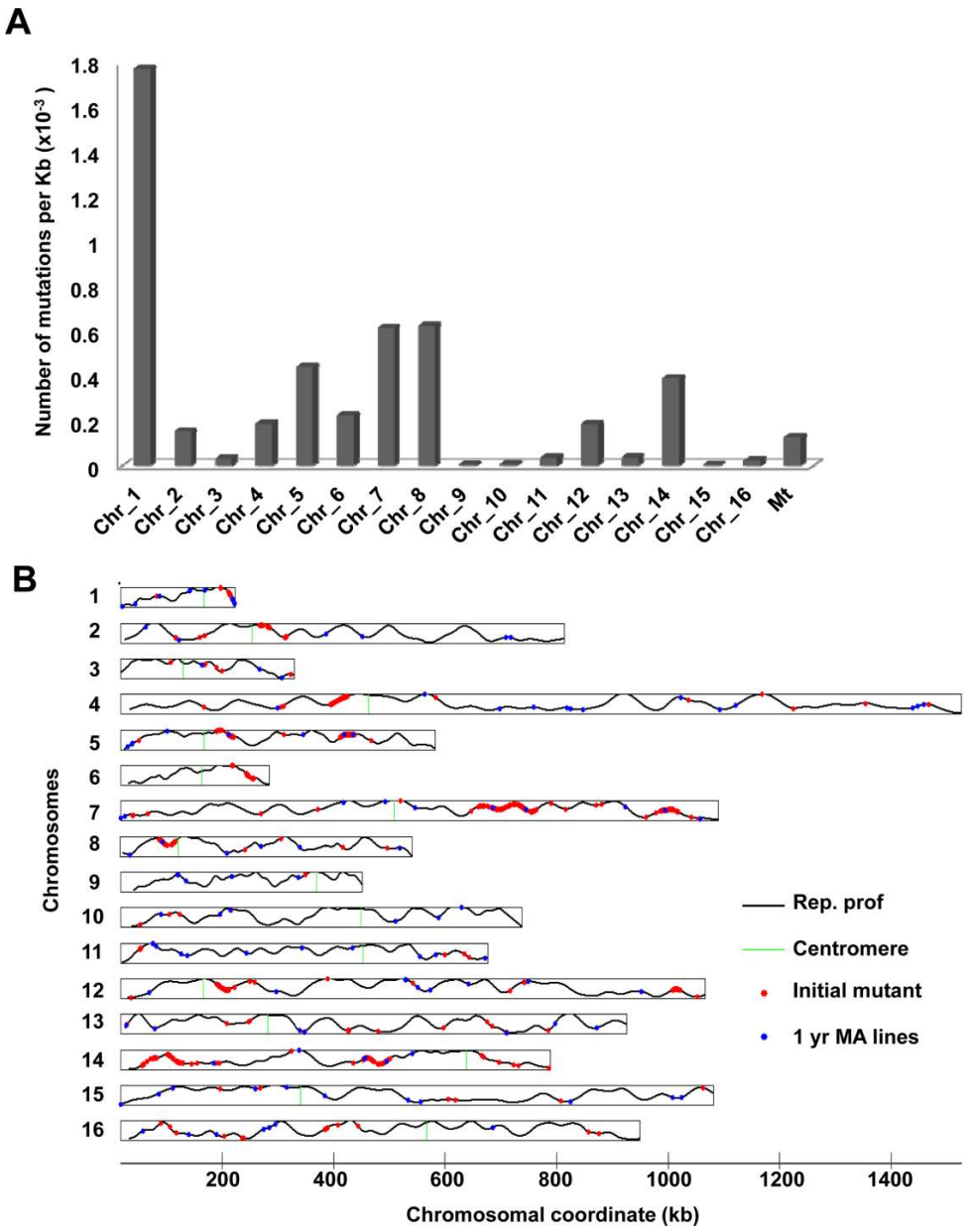

Figure S2. Chromosome distribution of mutations in the original Δ8 strain. A) Number of mutations was normalized according to chromosome length and plotted for each chromosome. **B**) Distribution of initial mutations (red dots) together with mutations identified after the long- term growth (blue dots) per chromosome shown with replication timing (Koren *et al*. 2010).

Table S2. Lifespan analysis of MA lines.

MA-line	MA-line Mean	MA-line N	Initial Mean	Initial N	% Change	Ranksum P-Value
1	4.4	20	9.2	20	52.2	0.011
2A	7	20	9.2	20	23.9	0.26
2B	6.9	20	9.2	20	25.0	0.23
3	6.3	20	9.2	20	31.5	0.14
4	4.3	20	9.2	20	53.3	0.011
5	6.4	20	9.2	20	30.4	0.13
6	6.4	20	9.2	20	30.4	0.13
Wt-1	15.8	20	20.7	20	23.7	0.11
Wt-2	16.6	20	20.7	20	19.8	0.13
Wt-3	19.8	20	20.7	20	4.6	0.79

Figure S3

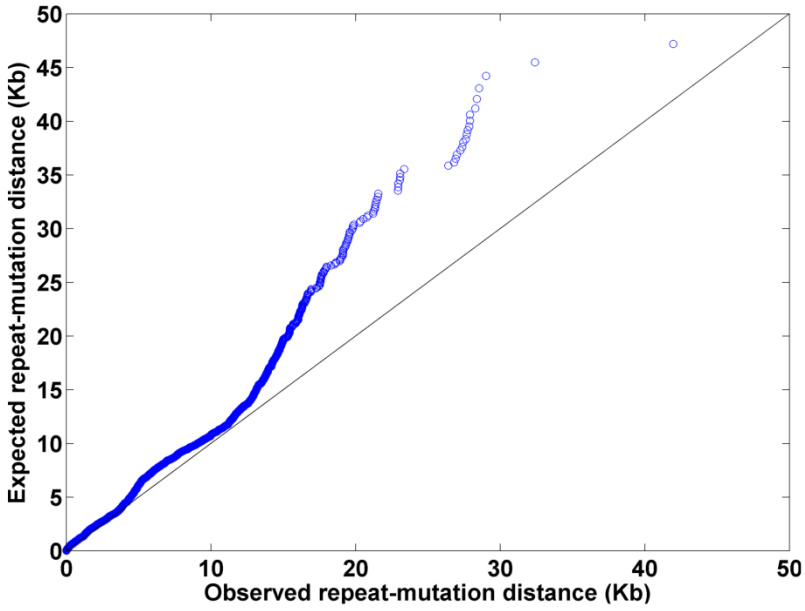

Figure S3. Observed versus expected distances between repeats and mutations in the initial Δ8 strain. Variable tandem repeats were extracted from Vinces *et al.* 2009 (intergenic repeats) and Verstrepen *et al.* 2005 (intragenic repeats) for our analysis. Blue circles are the observed versus expected distances between mutations in the initial strain and their nearest repeat. The expected distances between mutations and repeats were calculated by averaging over 100 randomized locations of mutations. The diagonal represents equal expected and observed distances. Only repeats of length of 5 bp or more and a repeat number of 3 or more were used for this analysis.

Table S3. Primers used for RNA-seq library preparation.

3‘ adapter	AppAGATCGGAAGAGCACACGTCT/3ddC/
RT-primer	pGATCGTCGGACTGTAGAACTCTGAACCTGTCGGTGGTCGCCGTATCATT/iSp18/GTGACTGGAGTTCAGACGTGTGCTCTTCCGATCT
PCR forward	AATGATACGGCGACCACCGACAGGTTCAGAGTTCTACAGTCCGACGATC
PCR reverse primers (indexed)	CAAGCAGAAGACGGCATACGAGAT**CGTGAT**GTGACTGGAGTTCAGACGTGTGCTCTTCCGATCT
	CAAGCAGAAGACGGCATACGAGAT**ACATCG**GTGACTGGAGTTCAGACGTGTGCTCTTCCGATCT
	CAAGCAGAAGACGGCATACGAGAT**GCCTAAG**TGACTGGAGTTCAGACGTGTGCTCTTCCGATCT
	CAAGCAGAAGACGGCATACGAGAT**TGGTCA**GTGACTGGAGTTCAGACGTGTGCTCTTCCGATCT
	CAAGCAGAAGACGGCATACGAGAT**CACTGT**GTGACTGGAGTTCAGACGTGTGCTCTTCCGATCT
	CAAGCAGAAGACGGCATACGAGAT**ATTGGC**GTGACTGGAGTTCAGACGTGTGCTCTTCCGATCT
	CAAGCAGAAGACGGCATACGAGAT**GATCTG**GTGACTGGAGTTCAGACGTGTGCTCTTCCGATCT
	CAAGCAGAAGACGGCATACGAGAT**TCAAGT**GTGACTGGAGTTCAGACGTGTGCTCTTCCGATCT
	CAAGCAGAAGACGGCATACGAGAT**CTGATC**GTGACTGGAGTTCAGACGTGTGCTCTTCCGATCT
	CAAGCAGAAGACGGCATACGAGAT**AAGCTA**GTGACTGGAGTTCAGACGTGTGCTCTTCCGATCT
	CAAGCAGAAGACGGCATACGAGAT**AAGCTA**GTGACTGGAGTTCAGACGTGTGCTCTTCCGATCT
	CAAGCAGAAGACGGCATACGAGAT**TACAAG**GTGACTGGAGTTCAGACGTGTGCTCTTCCGATCT

Figure S4

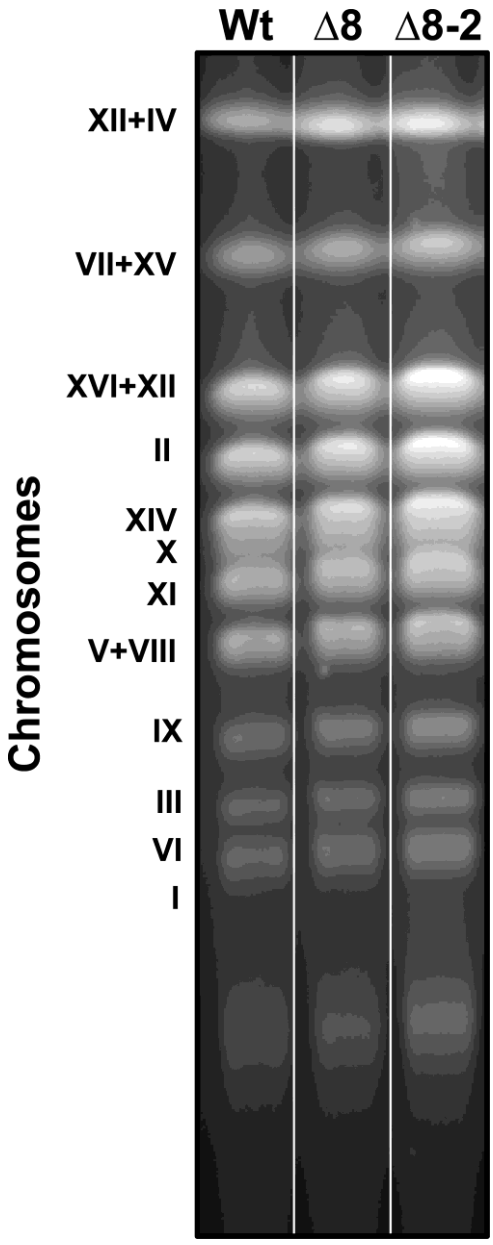

Figure S4. Pulse-field gel analysis showing chromosome size comparison between Wt and Δ8 isolates. PFGE was conducted using a BioRad Contour-clamped homogeneous electric field (CHEF) Mapper XA system and genomic samples were prepared using the CHEF genomic DNA plug kit. Agarose-embedded chromosomal DNA preparation and running conditions were performed according to the kit manual.

Figure S5

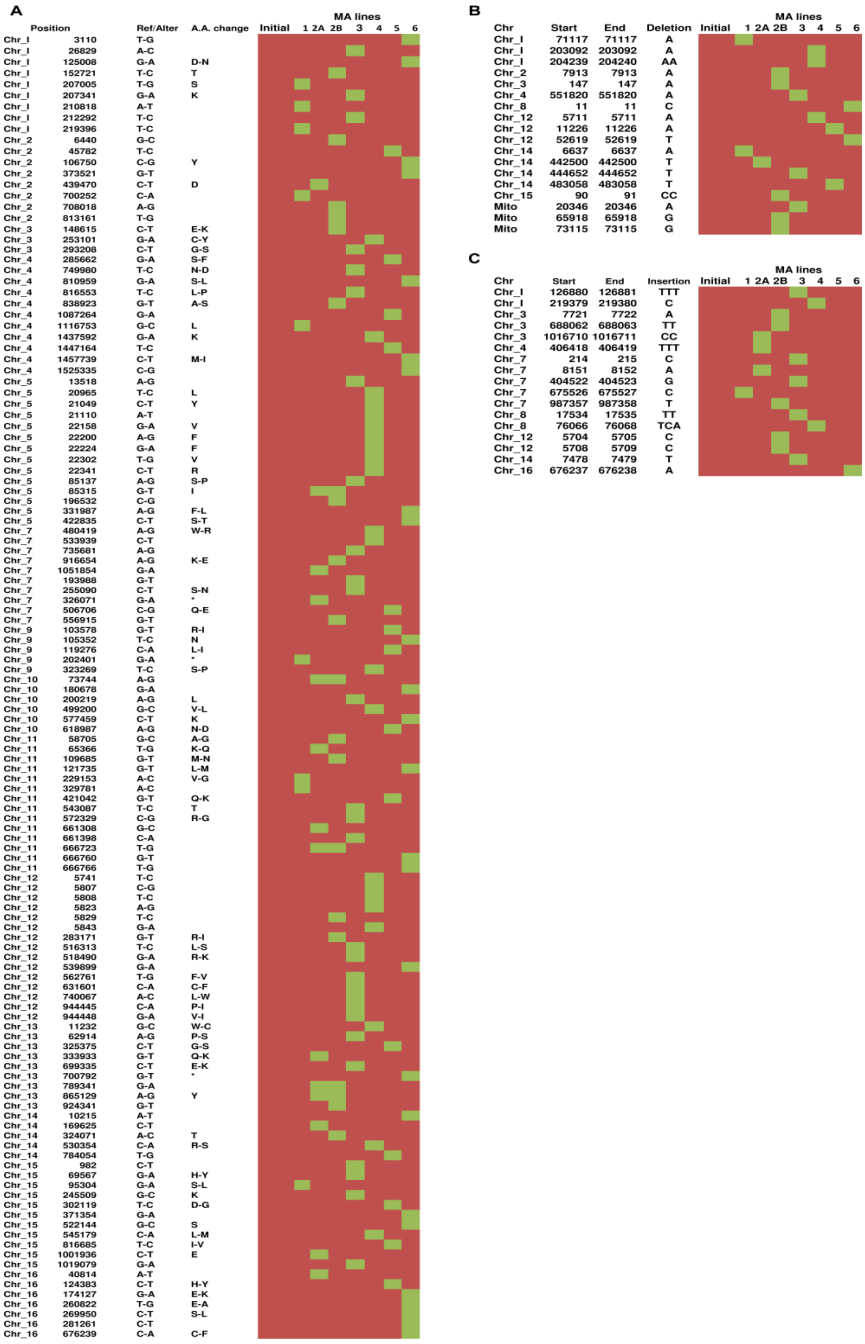

Figure S5. List of point mutations and indels in Δ8 MA lines following the long-term growth experiment. Green shows the presence of mutations with positions for each MA line represented by each column. Red shows the absence of mutations for this position for the indicated MA line. **A**) Point mutations. **B**) Deletions. **C**) Insertions.

Figure S6

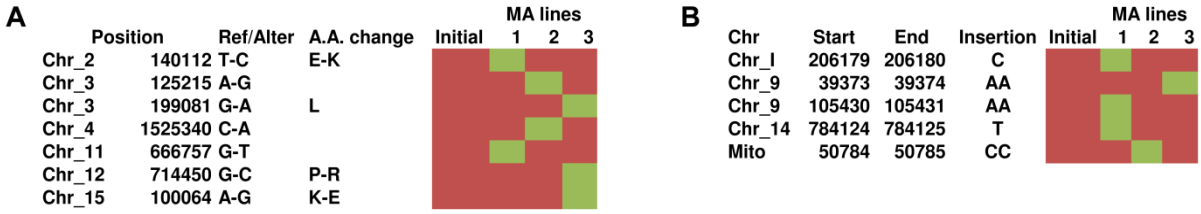

Figure S6. List of point mutations and indels in Wt MA lines following the long-term growth experiment. Same representation is shown here for Wt MA lines as in Figure S5.

Figure S7

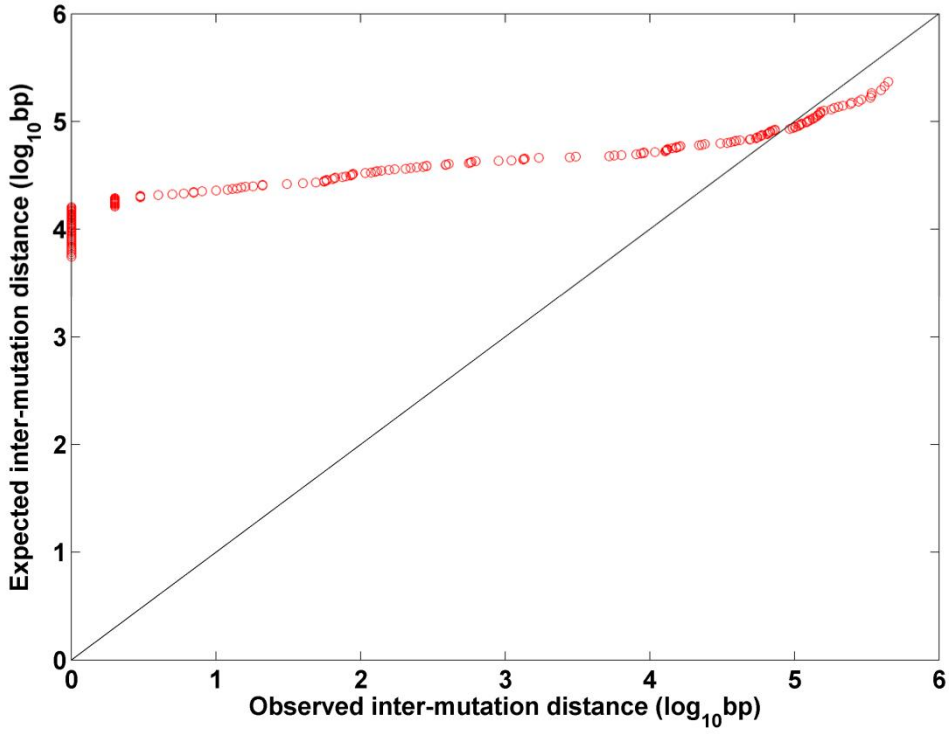

Figure S7. Clustering mutations in the new Δ8 isolate. Observed versus expected distances between adjacent mutations were analyzed as described in Figure 3B.

Figure S8

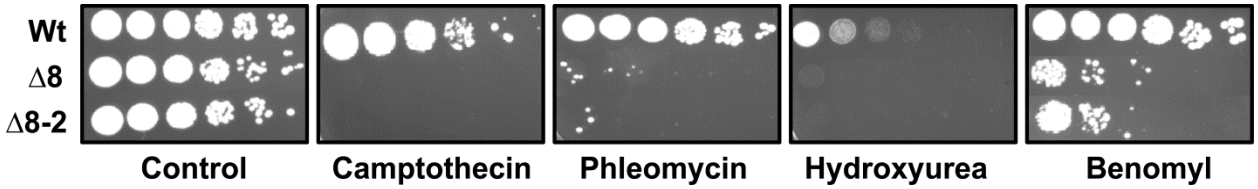

Figure S8. Sensitivity of Δ8 and Wt cells to DNA damage agents. Ten-fold dilution of Wt and Δ8 cells grown on YPD plates containing 15 µg/ml camptothecin (replication inhibitor), 150 mM hydroxyurea (replication inhibitor), 0.3 µg/ml phleomycine (double strand break inducer) or 15 µg/ml benomyl (microtubule poison).

Files S1-S2 are available for download as Excel files at http://www.genetics.org/lookup/suppl/doi:10.1534/genetics.114.169243/-/DC1.

File S1. List of mutations and indels in the initial Δ8 strains. Excel spreadsheet shows the position and nucleotide change of point mutations and indels in the Δ8 strains. If the mutation is in the coding region, gene was indicated on the right of the each position together with amino acid change. Genes without amino acid change indicates silent mutations.

File S2. List of genes and expression values analyzed in Wt and mutant strains. Log 2 value of each gene was clustered and analyzed to yield expression profile.

References

Koren, A., H. J. Tsai, I. Tirosh, L. S. Burrack, N. Barkai *et al*, 2010 Epigenetically-inherited centromere and neocentromere DNA replicates earliest in S-phase. PLoS Genet. **6:** e1001068.

Verstrepen, K. J., A. Jansen, F. Lewitter and G. R. Fink, 2005 Intragenic tandem repeats generate functional variability. Nat. Genet. **37:** 986-990.

Vinces, M. D., M. Legendre, M. Caldara, M. Hagihara and K. J. Verstrepen, 2009 Unstable tandem repeats in promoters confer transcriptional evolvability. Science **324:** 1213-1216.